Urologia Internationalis

Research Article

Urol Int 2021;105:875–890
DOI: 10.1159/000516676

Received: November 9, 2020
Accepted: April 16, 2021
Published online: July 7, 2021

Long Noncoding RNA LIPE-AS1 Drives Prostate Cancer Progression by Functioning as a Competing Endogenous RNA for microRNA-654-3p and Thereby Upregulating Hepatoma-Derived Growth Factor

Boyu Tian Chunxiang E. Yang Xiang Peng Teng

Department of Urology, The First Hospital of Qiqihar, Heilongjiang, China

Keywords
Competing endogenous RNA pathway · Hepatoma-derived growth factor · LIPE antisense RNA 1 · microRNA-654-3p · Prostate cancer

Abstract

Introduction: Information regarding the expression and roles of LIPE antisense RNA 1 (LIPE-AS1) in prostate cancer (PCa) progression is currently limited. We differentially determined LIPE-AS1 expression in tissues and cell lines. The specific functions of LIPE-AS1 in the oncogenicity of PCa were explored by evaluating a series of cellular functions. Moreover, the molecular mechanisms underlying the oncogenic roles of LIPE-AS1 in PCa were investigated. ***Methods:*** The expression level of LIPE-AS1 was determined via quantitative reverse transcription polymerase chain reaction. Functional experiments, including the Cell Counting Kit-8 assay, Transwell migration and invasion assays, and tumor xenograft experiments, were used to determine the effects of LIPE-AS1 on PCa cells. The putative miRNA-binding LIPE-AS1 was predicted via bioinformatics analysis and further verified using the luciferase reporter and RNA immunoprecipitation assays. ***Results:*** LIPE-AS1 was expressed at high levels in PCa cells; this result is consistent with that of The Cancer Genome Atlas database. Patients with PCa manifesting high LIPE-AS1 expression had shorter overall survival than those manifesting low LIPE-AS1 expression. Downregulated LIPE-AS1 inhibited PCa cell proliferation, migration, and invasion in vitro and impaired tumor growth in vivo. With respect to its mechanism, LIPE-AS1 functioned as a competing endogenous RNA for microRNA-654-3p (miR-654-3p) in PCa cells, and hepatoma-derived growth factor (HDGF) was the direct target of miR-654-3p. HDGF was positively regulated by LIPE-AS1 in PCa cells via the absorption of miR-654-3p. Rescue experiments confirmed that miR-654-3p downregulation or HDGF overexpression counteracts the inhibitory effects of LIPE-AS1 depletion on PCa cell proliferation, migration, and invasion. ***Conclusion:*** LIPE-AS1 promotes PCa malignancy by targeting the miR-654-3p/HDGF axis. Determining the LIPE-AS1/miR-654-3p/HDGF pathway may increase our understanding of PCa pathogenesis and contribute toward a wider applied scope.

Introduction

Globally, prostate cancer (PCa) is the most diagnosed malignancy in men [1], accounting for approximately 20% of the novel cancer cases in men [2]. Every year, 359,000 patients die due to PCa worldwide [3]. In the past

karger@karger.com
www.karger.com/uin

Correspondence to:
Peng Teng, urology_tengpeng@163.com

decade, there have been considerable advances in surgical techniques, endocrine therapy, hormonal agents, chemotherapy, and radiotherapy. As a result, the survival of patients with PCa has been significantly prolonged [4]. Nevertheless, a number of patients with PCa die within 5 years after primary diagnosis [5]. Furthermore, approximately 30% of patients with PCa experience relapse after conventional treatments [6, 7]. The complicated pathogenesis of PCa involves multiple factors, including age, lifestyle, environment, and heredity [8]. However, information regarding the mechanisms of PCa development is still limited [9]. Therefore, elucidating the mechanisms underlying the occurrence and development of PCa is urgently warranted, with the ultimate goal of identifying potential treatment strategies.

Long noncoding RNAs (lncRNAs) are defined as a subset of transcripts with >200 nucleotides that are not templates for protein synthesis [10]. lncRNAs are involved in the regulation of gene expression at the epigenetic, transcriptional, and posttranscriptional levels [11]. Existing studies have confirmed the vital functions of lncRNAs in a broad spectrum of physiological and pathological phenotypes [12]. Recently, the importance of lncRNAs in controlling prostate neoplasia and progression has been widely acknowledged [13]. Many lncRNAs are aberrantly expressed and perform crucial regulatory actions in PCa, proving their potential as novel therapeutic targets.

MicroRNAs (miRNAs) are a category of short non-coding RNAs containing 17–25 nucleotides [14]. They exert important roles in controlling gene expression by base-pairing with the 3′-untranslated regions of downstream target genes and forming a silencing complex, resulting in translation inhibition or target mRNA degradation [14]. Although miRNAs can be translated into proteins, they are involved in various pathological processes, including cancer oncogenesis and progression [15]. Several studies have revealed that miRNAs are dysregulated in PCa and execute oncogenic or anti-oncogenic roles during PCa progression [16]. Several studies have recently reported that competing endogenous RNA (ceRNA) networks play an important role in human cancers [17]. Briefly, lncRNAs carry one or more miRNA response elements and can sponge certain miRNAs, thereby upregulating the expression of the miRNA targets [18]. Considering the important roles of lncRNAs and miRNAs, we aimed to further investigate their expression, roles, and possible mechanisms in PCa.

Numerous lncRNAs have been identified in the human genome; yet, there are still many lncRNAs whose expression and exact roles remain largely unknown in PCa and require further elucidation. Through The Cancer Genome Atlas (TCGA) database, we found that LIPE antisense RNA 1 (LIPE-AS1) was one of the most differentially expressed lncRNAs. Therefore, the present study aimed to investigate the detailed roles and probable molecular mechanisms of LIPE-AS1 in PCa in order to improve our understanding of its pathogenesis and contribute toward a wider application scope. First, we investigated the expression pattern of LIPE-AS1 in PCa and characterized its clinical significance. Then, we explored the detailed roles of LIPE-AS1 in the oncogenicity of PCa by evaluating a series of cellular functions. Finally, we investigated the molecular mechanisms underlying the oncogenic roles of LIPE-AS1 in PCa.

Materials and Methods

Tissue Collection

Fifty-two pairs of PCa tissues and adjacent normal tissues were collected from patients with PCa at the First Affiliated Hospital of Qiqihar Medical University. Pathologists confirmed the tumor cell content of PCa tissues. None of the patients underwent local or systemic anticancer therapy before their enrollment into this study. All tissues were stored in liquid nitrogen until use. This study was approved by the Medical Ethics Committee of the First Affiliated Hospital of Qiqihar Medical University and was conducted in full accordance with the World Medical Association's Declaration of Helsinki. All participants signed an informed consent document before the study. The clinical and histopathological information of all PCa patients are summarized in Table 1.

TCGA Program

The TCGA dataset of PCa (TCGA-PRAD) was downloaded from the TGCA Data Portal (https://tcga-data.nci.nih.gov/tcga/). The database contained 498 PCa tissues and 51 normal tissues. These cohorts were used for RNA expression analysis of LIPE-AS1 and miR-654-3p. Also, the clinical value of miR-654-3p in patients with PCa was analyzed in the cohorts.

Cell Culture

Two PCa cell lines, namely, LNCaP and 22RV1, were purchased from the Type Culture Collection of the Chinese Academy of Sciences (Shanghai, China) and maintained in Roswell Park Memorial Institute medium 1640 supplemented with 10% fetal bovine serum (FBS) and 1% sodium pyruvate (Gibco; Thermo Fisher Scientific, Inc., Waltham, MA, USA). Another PCa cell line, DU145 (Type Culture Collection of the Chinese Academy of Sciences), was cultured in Dulbecco's modified Eagle's medium (Gibco; Thermo Fisher Scientific, Inc.) with 10% FBS. RWPE-1, a normal human prostate epithelial cell line, was also obtained from the Type Culture Collection of the Chinese Academy of Sciences and maintained in Keratinocyte-SFM medium (Gibco; Thermo Fisher Scientific, Inc.) supplemented

Table 1. Clinical and histopathological information of all PCa patients

No.	Age, years	PSA, ng/mL	Gleason score	Metastasis	No.	Age, years	PSA, ng/mL	Gleason score	Metastasis
1	54	16.88	4 + 3	Negative	27	60	29.52	5 + 4	Positive
2	66	25.65	4 + 3	Negative	28	69	26.83	4 + 4	Negative
3	57	20.15	5 + 4	Negative	29	72	15.20	5 + 4	Negativ
4	73	10.26	5 + 3	Negative	30	70	23.53	4 + 3	Negati
5	68	27.59	4 + 4	Positive	31	58	25.62	4 + 4	gativ
6	59	23.73	4 + 3	Negative	32	63	18.46	5 + 4	ive
7	71	16.32	5 + 4	Negative	33	55	23.44	4 + 4	Po
8	55	21.85	4 + 3	Negative	34	71	28.70	4 + 3	Nega
9	57	14.47	5 + 4	Negative	35	65	10.93	3	Negativ
10	74	16.87	5 + 4	Negative	36	68	28.91	+ 3	ive
11	70	31.25	4 + 4	Negative	37	62	17.02	4	itive
12	68	22.68	4 + 5	Negative	38	54	23.47	+ 3	Negative
13	73	27.31	5 + 4	Negative	39	67	12.75	+ 3	Negative
14	65	23.14	5 + 4	Negative	40	70	26.80	4	Negative
15	69	17.68	4 + 4	Negative	41	65	15.32		Negative
16	58	21.42	5 + 3	Negative	42	68	26.8	5 +	Positive
17	59	30.04	4 + 3	Positive	43	57	11.20	4 + 3	Negative
18	74	26.20	3 + 3	Negative	44	62	18.64	4 + 3	Negative
19	67	27.35	4 + 3	Negative	45	70	8	5 + 4	Negative
20	70	29.18	5 + 4	Negative	46	61		4 + 3	Negative
21	56	16.78	5 + 4	Negative	47	68	.78	5 + 4	Negative
22	74	23.19	4 + 5	Negative	4	59	13.55	5 + 3	Negative
23	72	18.06	4 + 4	Negative		57	2.17	4 + 3	Negative
24	57	25.53	5 + 4	Negative	50	65	35.09	5 + 4	Positive
25	65	12.00	4 + 3	Negative	5		23.42	5 + 4	Negative
26	68	27.38	5 + 4	Negative			16.77	4 + 3	Negative

PSA, prostate-specific antigen; PCa, prostate cancer.

with a gentamicin and amphotericin solution (Thermo Fisher Scientific, Inc.). All cells were grown at 37°C in a humidified incubator with 5% CO_2.

Cell Transfection

Small interfering RNAs (siRNAs) against LIPE-AS1 (si-LIPE-AS1#1, si-LIPE-AS1#2, and si-LIPE-AS1#3) and negative control (NC) siRNA (si-NC) were designed and purchased from Genepharma Co., Ltd. (Shanghai, China). A nonsense sequence (si-NC) was used as the control. The si-LIPE-AS1#1 sequence was 5′-GAGTTTTTAAATAAATAGATA-3′; the si-LIPE-AS1#2 sequence was 5′-TCACTTTGAATCAAACTCT-3′; the si-LIPE-AS1#3 sequence was 5′-GCCAAGACAACATAAACAAGAGC-3′; and the NC sequence was 5′-CACGATAAGACAATC-3′. The HDGF overexpression plasmid was constructed by inserting the HDGF sequence into the pcDNA3.1 plasmid to form pcDNA3.1-HDGF (Guangzhou RiboBio Co., Ltd., Guangzhou, China). miR-654-3p mimic and miR-654-3p inhibitor (anti-miR-654-3p) were obtained from RiboBio Co., Ltd. The mimic and NC inhibitor (anti-NC) functioned as the respective controls. One night prior to transfection, PCa cells were seeded into 6-well plates. Cells were transfected with the aforementioned siRNAs (100 pmol), miRNA mimic (100 pmol), miRNA inhibitor (100 pmol), or plasmids (4 μg) using Lipofectamine® 2000 (Invitrogen; Thermo Fisher Scientific, Inc.). After 48 h of transfection, quantitative reverse transcription polymerase chain reaction (qRT-PCR), Cell Counting Kit-8 (CCK-8) assay, and Western blotting were performed. Transwell migration and invasion assay and Western blotting were implemented at 24 h post-transfection.

Quantitative Reverse Transcription Polymerase Chain Reaction

Total RNA was extracted from the tissues or cells using the TRIzol reagent (Beyotime Institute of Biotechnology, Shanghai, China). The quality and quantity of total RNA were determined using the Nanodrop 2000 system (Invitrogen; Thermo Fisher Scientific, Inc.). To quantify the expression levels of LIPE-AS1 and HDGF, qRT-PCR was performed using the PrimeScript® RT reagent Kit (Takara, Dalian, China) and SYBR® Premix Ex TaqTM II (Takara). To determine miRNA expression, the Mir-X miRNA First-Strand Synthesis Kit (Takara) was used to reverse transcribe total RNA. Quantitative PCR was performed using the Mir-X miRNA qRT-PCR TB Green® Kit (Takara). Glyceraldehyde-3-phosphate dehydrogenase (GAPDH) was used as the control for LIPE-AS1 and HDGF, and miRNA expression was normalized to that of U6 small nuclear RNA. Relative gene expression was determined using the $2^{-\Delta\Delta Ct}$ method. The primer sequences are shown in Table 2.

Table 2. Primers sequences for qRT-PCR

Gene	Sequences (5′ → 3′)
LIPE-AS1	
Forward	GAGTTAACGGTGAAGTCCACAAAA
Reverse	AAAAATCTATACCTCACAGTTCGGG
HDGF	
Forward	GATCGAGAACAACCCTACTGTCAA
Reverse	GCATTCCCCTTCTTATCACCG
GAPDH	
Forward	AGTCAACGGATTTGGTCGTATTG
Reverse	AAACCATGTAGTTGAGGTCAATGAA
miR-760	
Forward	TCGGCAGGCGGCUCUGGG
Reverse	CACTCAACTGGTGTCGTGGA
miR-654-3p	
Forward	TCGGCAGGCGUGUACAAGACGC
Reverse	CACTCAACTGGTGTCGTGGA
miR-642a-5p	
Forward	TCGGCAGGGUCCCUCUCCAAAUG
Reverse	CACTCAACTGGTGTCGTGGA
miR-520a-5p	
Forward	TCGGCAGGCUCCAGAGGGAAGU
Reverse	CACTCAACTGGTGTCGTGGA
miR-455-3p	
Forward	TCGGCAGGCACAUAUACGGGU
Reverse	CACTCAACTGGTGTCGTGGA
miR-424-5p	
Forward	TCGGCAGGCAGCAGC[illegible]AUUC[illegible]
Reverse	CACTCAACTGGTGTC[illegible]A
miR-330-5p	
Forward	TCGGCAGGUCUC[illegible]GGC[illegible]
Reverse	CACTCAACTGGT[illegible]CGTGGA
miR-326	
Forward	TCGGCA[illegible]GGC[illegible]GCCU
Reverse	CACTC[illegible]GTCGTGGA
miR-299-3p	
Forward	T[illegible]CAC[illegible]GCCAAAUGGU
Reverse	[illegible]CAACTGGTGTCGTGGA
miR-107	
Forward	TCGG[illegible]AGGAGCAGCAUUGUAC
Reverse	[illegible]CAACTGGTGTCGTGGA
U6	
Forwa[illegible]	CTCGCTTCGGCAGCACA
[illegible]vers[illegible]	AACGCTTCACGAATTTGCGT

[illegible]-PCR, quantitative reverse transcription polymerase chain [illegible]ac[illegible]

Subcellular Fractionation

PCa cells were treated with the Nuclear/Cytosol Fractionation Kit (Biovision, San Francisco, CA, USA) to obtain the nuclear and cytoplasmic fractions. After RNA extraction, the level of LIPE-AS1 in the cytoplasm and nucleus of PCa cells was examined via qRT-PCR. U6 and GAPDH were used as the internal nuclear and cytoplasmic references, respectively.

CCK-8 Assay

PCa cells were transfected for 24 h and then ha[illegible]d a[illegible] seeded into 96-well plates. Each well contained 1[illegible]μL [illegible] cell suspension containing 2×10^3 cells. The CCK-8 [illegible]jindo M[illegible] lar Technologies, Inc., Kumamoto, J[illegible]an) wa[illegible]d to study cell proliferation. At 0, 1, 2, and 3 days a[illegible]r cell in[illegible]μL of the CCK-8 reagent was added into ea[illegible]ll, a[illegible]ells were incubated at 37°C for an additi[illegible]h. [illegible]tical density was detected at a wavelength of 450 [illegible]ng a m[illegible]late reader.

Transwell Migration and [illegible]asion

The migration and i[illegible]e abilities [illegible] PCa cells were determined using the 24-well T[illegible]ell insert system (Corning Costar, Corning, NY[illegible] Transfe[illegible]Ca cells were collected, rinsed with phosp[illegible]-b[illegible]olutio[illegible]and resuspended in culture medium witho[illegible]S. A[illegible]liquot of the cell suspension containing 5×10^4[illegible] se[illegible]d into the upper Transwell chambers. [illegible]e culture me[illegible] supplemented with 20% FBS served as the [illegible]oattractant a[illegible]as added to the basolateral Transwell cham-be[illegible]coated wi[illegible]out (for migration) or with (for invasion) [illegible]D Biosciences, San Jose, CA, USA). After culturing the [illegible]lls fo[illegible] nonmigrated or noninvaded cells were removed us-[illegible] w[illegible]otton bud. Migrated or invaded cells were fixed using [illegible]hanol and dyed with 0.1% crystal violet. The stained cells were photographed under a light microscope (×200 magnification; [illegible]lympus, Tokyo, Japan). The number of migrated or invaded cells [illegible]as counted in 5 randomly selected fields.

Tumor Xenograft Experiments

All animal procedures were approved by the Animal Care and Use Committee of the First Affiliated Hospital of Qiqihar and conducted in compliance with the recommended procedures of the National Institutes of Health guidelines for the care and use of laboratory animals. The short hairpin RNA against the expression of LIPE-AS1 (sh-LIPE-AS1) and the NC short hairpin RNA (sh-NC) were designed and produced by Genepharma Co., Ltd., and cloned into a lentiviral plasmid. The sh-LIPE-AS1 sequence was 5′-CCGGGCCAAGACAACATAAACAAGACCCTCGAGGC-CAAGACAACATAAACAAGACCTTTTTG-3′; and the sh-NC sequence was 5′-CCGGCACGATAAGACAATGTATTTCTC-GAGAAATACATTGTCTTATCGTGTTTTTG-3′. The plasmid was transfected into 293T cells along with lentiviral packaging plasmids. The supernatants carrying sh-LIPE-AS1 or sh-NC lentivirus were collected after 3 days of incubation and used to infect DU145 cells. DU145 cells stably overexpressing sh-LIPE-AS1 or sh-NC were selected using 0.5 μg/mL puromycin.

Male BALB/c nude mice aged 4–6 weeks were purchased from Shanghai SLAC Laboratory Animal, Co., Ltd. (Shanghai, China) and subcutaneously injected with 1×10^6 DU145 cells stably overexpressing sh-LIPE-AS1 or sh-NC. Each group contained 3 nude mice. One week after cell inoculation, the tumor volume was monitored every 5 days. The tumor volume was calculated using the

following formula: 0.5 × length × width^2. After 32 days, mice were euthanized via cervical dislocation, and tumor xenografts were excised for weight assessment and further use.

Bioinformatics Prediction

The potential miRNA targets of sh-LIPE-AS1 were identified using StarBase 3.0 (http://starbase.sysu.edu.cn/). TargetScan (http://www.targetscan.org/) and miRDB (http://mirdb.org/) were used to predict the potential targets of miR-654-3p.

Luciferase Reporter Assay

Fragments of LIPE-AS1 and HDGF containing the wild-type (wt) or mutant (mut) miR-654-3p-binding sites were constructed by Genepharma Co., Ltd., and inserted into the pmirGLO Dual-Luciferase Reporter Vector (Promega, Madison, WI, USA) to generate the reporter plasmids LIPE-AS1-wt, LIPE-AS1-mut, HDGF-wt, and HDGF-mut. For reporter assays, miR-654-3p mimic or NC mimic was cotransfected with the wt or mut reporter plasmids using Lipofectamine 2000. The culture was maintained at 37°C for 48 h, followed by the detection of luciferase activity using the Dual-Luciferase Reporter Assay System (Promega).

RNA Immunoprecipitation Assay

The interaction between LIPE-AS1, miR-654-3p, and HDGF in PCa cells was verified using the Magna RIP™ RNA-Binding Protein Immunoprecipitation Kit (Millipore, Billerica, MA, USA). PCa cells were lysed in RNA immunoprecipitation (RIP) lysis buffer, and cell extracts were collected for the RIP assay. A volume of 10 μL of the cell extract was defined as the input. The cell extracts (100 μL) were probed with RIP buffer containing magnetic beads conjugated with human anti-Ago2 antibody or normal mouse immunoglobulin G (IgG; Millipore). After overnight incubation at 4°C, the magnetic beads were collected and treated with proteinase K at 55°C for 30 min. After the immunoprecipitated RNA was extracted, qRT-PCR was performed to determine the enrichment of LIPE-AS1, miR-654-3p, and HDGF.

RNA Pull-Down Assay

The assay was implemented to further confirm the binding interaction between LIPE-AS1 and miR-654-3p in PCa cells. The biotinylated miR-654-3p mimic (bio-miR-654-3p), biotinylated NC mimic (bio-NC) was prepared using the Pierce™ Biotin 3′ End DNA Labeling Kit (Thermo Fisher Scientific, Inc.). After transfection with biotinylated RNA, PCa cells were incubated at 37°C in a humidified incubator with 5% CO_2 for 48 h. Thereafter, transfected cells were collected and probed with the precooled lysis buffer. After centrifugation, the supernatant was further cultivated with Dynabeads M-280 Streptavidin (BD Biosciences) at 4°C for additional 2 h, generating the bio-miRNA-lncRNA complexes. Finally, qRT-PCR was conducted to test the relative enrichment of LIPE-AS1 and miR-654-3p in the yield complexes.

Western Blot Analysis

Cells were solubilized using RIP assay buffer (Beyotime Institute of Biotechnology). Then, the isolated protein was quantified using a BCA Protein Assay Kit (Beyotime Institute of Biotechnology). Equivalent amounts of protein were separated via 10% sodium dodecyl sulfate-polyacrylamide gel electrophoresis and transferred onto polyvinylidene difluoride membranes. After 2 h of blocking with 5% nonfat milk at room temperature, the primary antibodies targeting HDGF (ab128921; 1:1,000 dilution; Abcam, Cambridge, MA, USA) or GAPDH (ab128915; 1:1,000 dilution; Abcam) were added to the membrane, followed by overnight incubation at 4°C. Upon probing the membrane with goat anti-rabbit horseradish peroxidase-conjugated IgG secondary antibody (ab205718; 1:5,000 dilution; Abcam) at room temperature for 2 h, the protein bands were visualized using the Immobilon Western Chemiluminescent HRP substrate (Millipore, Billerica, MA, USA). Densitometry was performed applying Quantity One software version 4.62 (Bio Rad Laboratories, Inc., Hercules, CA, USA).

Statistical Analyses

All experiments were repeated 3 times, and each experiment was performed in triplicate. All statistical analyses were conducted using SPSS 20.0 (IBM SPSS, Armonk, NY, USA). Student's *t* test was used for between-group comparisons. The differences in multiple groups were evaluated via the one-way ANOVA with Tukey's post hoc test. Pearson correlation analysis was performed to assess the correlation between LIPE-AS1, miR-654-3p, and HDGF levels. All results are expressed as mean ± standard deviation, and a significant difference was considered when p was <0.05.

Results

LIPE-AS1 Downregulation Inhibits PCa Cell Proliferation, Migration and Invasion

LIPE-AS1 expression in PCa was first evaluated using the TCGA database. Compared with normal tissues, LIPE-AS1 expression was upregulated in PCa tissues (shown in Fig. 1a). Then, 52 pairs of PCa tissues and adjacent normal tissues were collected and used to quantify LIPE-AS1 expression via qRT-PCR. qRT-PCR revealed that LIPE-AS1 expression was higher in PCa tissues than that in adjacent normal tissues (shown in Fig. 1b). Furthermore, LIPE-AS1 was overexpressed in PCa cell lines (LNCaP, 22RV1, and DU145) compared with the normal human prostate epithelial cell line RWPE-1 (shown in Fig. 1c). Importantly, the overall survival of PCa patients manifesting high LIPE-AS1 expression was lower than those manifesting low LIPE-AS1 expression (shown in Fig. 1d).

Considering the relatively high LIPE-AS1 levels in 22RV1 and DU145 cells, these 2 cell lines were selected for follow-up experiments. To explore the biological role of LIPE-AS1 in PCa, si-LIPE-AS1 was transfected into 22RV1 and DU145 cells to knockdown LIPE-AS1 expression (shown in Fig. 1e). The CCK-8 assay revealed that silencing LIPE-AS1 expression decreased the proliferation of 22RV1 and DU145 cells (shown in Fig. 1f). Moreover, the Transwell migration and invasion assays revealed that LIPE-AS1 suppression decreased the migration (shown in Fig. 1g) and invasive (shown in Fig. 1h)

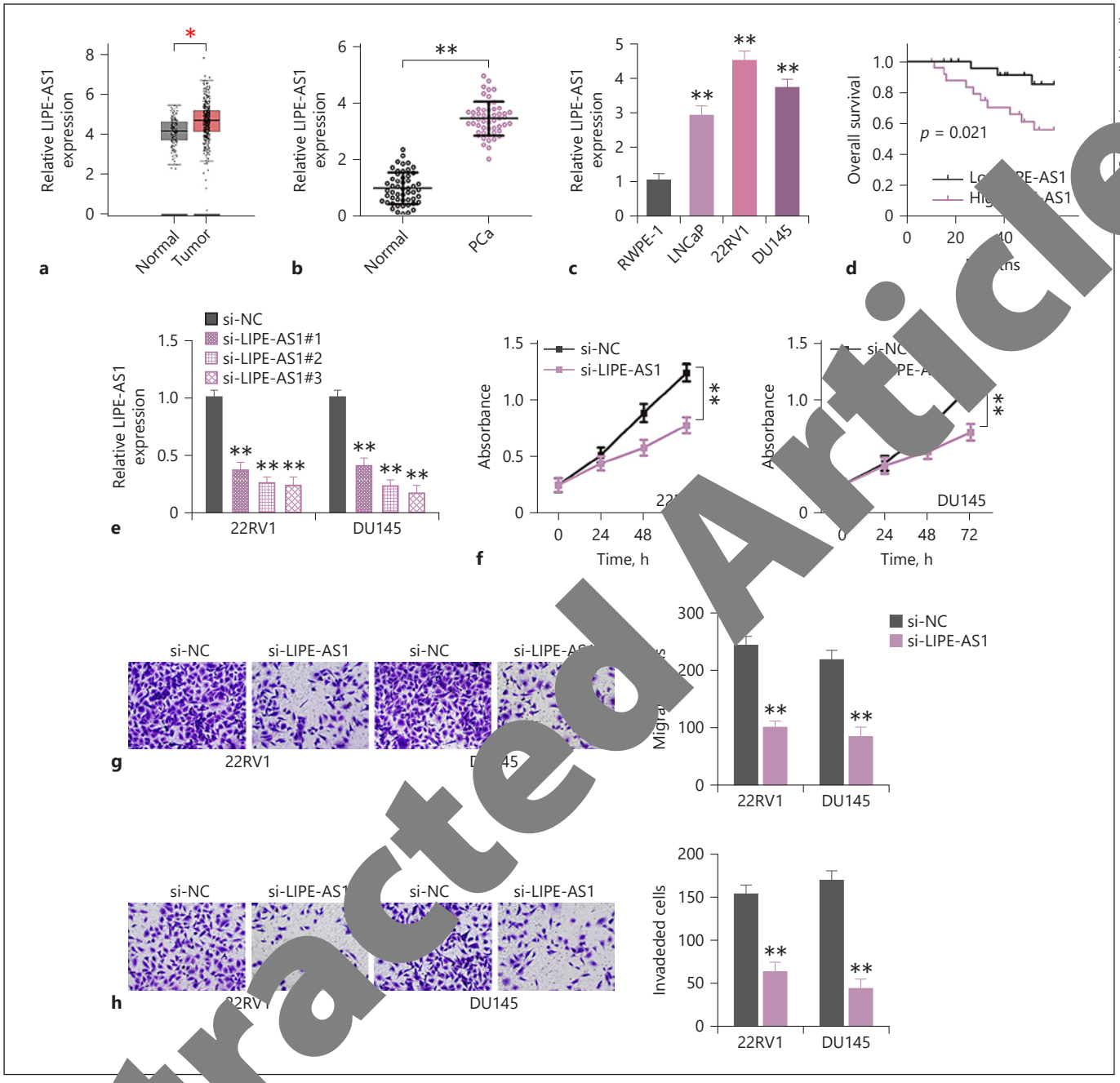

Fig. 1. LIPE-A[illegible]letion i[illegible]oits PCa cell proliferation, migration, and invasion. [illegible]database was used to analyze LIPE-AS1 expressi[illegible]Ca tis[illegible] qRT-PCR was performed to assess LIPE-AS[illegible]xpr[illegible]on in 52 pairs of PCa tissues and adjacent normal tissues[illegible]exp[illegible]sion levels of LIPE-AS1 in 3 PCa cell lines (LNCaP, 22[illegible]DU145) and a normal human prostate epithelial [illegible]line RW[illegible]E-1 were detected via qRT-PCR. **d** The log-rank test [illegible]ucted to examine the overall survival rate of PCa tissues based[illegible]high or low LIPE-AS1 levels. **e** LIPE-AS1 expression was determined via RT-qPCR in 22RV1 and DU145 cells transfected with siRNAs against LIPE-AS1. **f** The CCK-8 assay presented the proliferation ability of 22RV1 and DU145 cells when LIPE-AS1 was silenced. **g**, **h** The migration and invasive abilities of PCa cells were assessed using the Transwell migration and invasion assays after LIPE-AS1 silencing (×200 magnification). $^{**}p < 0.01$. TCGA, The Cancer Genome Atlas; qRT-PCR, quantitative reverse transcription polymerase chain reaction; CCK-8, Cell Counting Kit 8; PCa, prostate cancer; LIPE-AS1, LIPE antisense RNA 1.

abilities of 22RV1 and DU145 cells. Taken together, these results demonstrate that LIPE-AS1 exhibits tumor-promoting roles in PCa cells.

LIPE-AS1 Acts as an miR-654-3p Decoy in PCa Cells

After identifying the roles of LIPE-AS1 in PCa cells, we elucidated the molecular events underlying the oncogenic roles of LIPE-AS1. First, lncLocator (http://www.csbio.sjtu.edu.cn/bioinf/lncLocator/) was used to predict the subcellular location of LIPE-AS1. LIPE-AS1 was predicted to primarily exist in the cytoplasm (shown in Fig. 2a). Simultaneously, the subcellular fractionation assay confirmed the major distribution of LIPE-AS1 in the cytoplasm of 22RV1 and DU145 cells (shown in Fig. 2b). Therefore, we speculated that LIPE-AS1 functions as a ceRNA in PCa by acting as a decoy for specific miRNAs, thereby modulating gene expression at the posttranscriptional level.

Using StarBase 3.0, 54 miRNAs possessing binding sites for LIPE-AS1 were identified. TCGA database was used to analyze the expression statuses of these miRNAs in PCa tissues. Ten miRNAs were found to be weakly expressed in PCa tissues (shown in Fig. 2c). Then, qRT-PCR was conducted to determine the expression levels of these miRNAs in 22RV1 and DU145 cells after LIPE-AS1 knockdown. The results revealed that only miR-654-3p expression increased in LIPE-AS1-deficient 22RV1 and DU145 cells, whereas the expression levels of the other miRNAs remained unchanged in response to LIPE-AS1 knockdown (shown in Fig. 2d). In addition, miR-654-3p expression demonstrated a decreasing trend in PCa tissues compared with that in adjacent normal tissues (shown in Fig. 2e). Pearson's correlation analysis verified that LIPE-AS1 expression was inversely related to miR-654-3p expression in 52 PCa tissues (shown in Fig. 2f). The predicted binding sites between LIPE-AS1 and miR-654-3p is shown in Figure 2g. The luciferase reporter assay was then performed to further investigate the interaction between LIPE-AS1 and miR-654-3p in PCa cells. The results revealed that miR-654-3p overexpression significantly reduced the luciferase activity of LIPE-AS1-wt but not that of LIPE-AS1-mut in 22RV1 and DU145 cells (shown in Figure 2h).

AGO2 is a core element of RNA-induced silencing complexes and can directly induce the degradation of target RNAs via its catalytic activity in gene silencing processes produced by siRNAs or miRNAs. Thus, the RIP assay was conducted using human anti-Ago2 antibody. As shown in Figure 2i, LIPE-AS1 and miR-654-3p were highly enriched in the anti-Ago2 group than in the control IgG group, confirming the association between LIPE-AS1 and miR-654-3p in the same RNA-induced silencing complexes. Furthermore, the RNA pull-down assay demonstrated that the relative LIPE-AS1 enrichment was higher in the bio-miR-654-3p group than that in the bio-NC group, further certifying that LIPE-AS1 is bound to miR-654-3p directly (shown in Fig. 2j). Taken together, the results suggest that LIPE-AS1 acts as an miR-654-3p decoy in PCa cells.

HDGF Is the Direct Target of miR-654-3p in PCa Cells

Considering the downregulation of miR-654-3p in PCa tissues (shown in Fig. 3a), we explored the clinical value of miR-654-3p in PCa using the TCGA database. Decreased miR-654-3p expression was closely correlated with age (shown in Fig. 3b), Gleason score (shown in Fig. 3c), and lymph node metastasis (shown in Fig. 3d) in patients with PCa. Using our own cohort, downregulation of miR-654-3p also presented a notable correlation with age (shown in Fig. 3e), Gleason score (shown in Fig. 3f), and lymph node metastasis (shown in Fig. 3g) in patients with PCa.

To identify the roles of miR-654-3p in PCa, 22RV1, DU145, cells were transfected with the miR-654-3p mimic or NC mimic; the transfection efficiency was assessed via qRT-PCR. Transfection with the miR-654-3p mimic led to the notable overexpression of miR-654-3p in 22RV1 and DU145 cells (shown in Fig. 4a). The CCK-8 assay results indicated that compared with the NC mimic group, the proliferative ability of 22RV1 and DU145 cells was remarkably suppressed after miR-654-3p mimic transfection (shown in Fig. 4b). Furthermore, ectopic miR-654-3p expression decreased the migration (shown in Fig. 4c) and invasion (shown in Fig. 4d) of 22RV1 and DU145 cells. Bioinformatics analysis was performed to determine the target of miR-654-3p. HDGF (shown in Fig. 4e) was selected for further experimental verification due to its important regulatory roles in PCa. The mRNA expression level of HDGF was upregulated in PCa tissues compared with that in adjacent normal tissues (shown in Fig. 4f). A negative correlation was observed between HDGF and miR-654-3p expression in 52 PCa tissues (shown in Fig. 4g) via Pearson's correlation analysis. To confirm this relationship, mRNA and protein levels of HDGF were determined in miR-654-3p mimic-transfected 22RV1 and DU145 cells. The increased expression of miR-654-3p suppressed the expression of HDGF in 22RV1 and DU145 cells at both the mRNA (shown in Fig. 4h) and protein (shown in Fig. 4i) levels. Eventually, the luciferase re-

porter assay revealed that miR-654-3p overexpression decreased the luciferase activity of the HDGF-wt reporter plasmid in 22RV1 and DU145 cells but not that of the HDGF-mut (shown in Fig. 4j). Taken together, these results indicate that HDGF is the direct target of miR-654-3p in PCa cells.

LIPE-AS1 Functions as a ceRNA by Sponging miR-654-3p to Increase HDGF Expression

A series of mechanistic experiments were conducted to address whether LIPE-AS1 functions as a ceRNA to regulate the miR-654-3p/HDGF axis. The mRNA (shown in Fig. 5a) and protein (shown in Fig. 5b) expression levels of HDGF were decreased in LIPE-AS1 transfected 22RV1 and DU145 cells. The RI

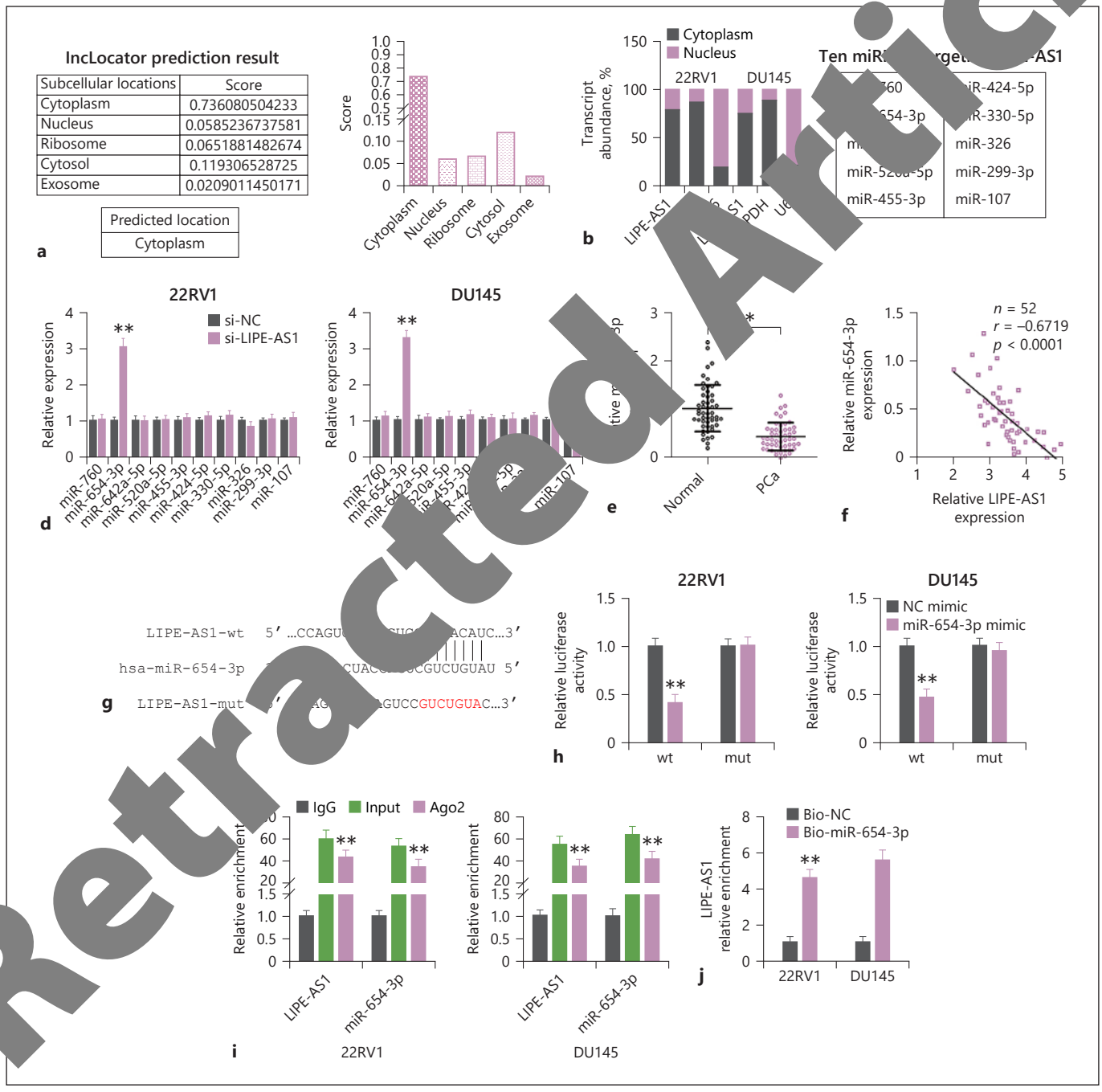

2

(For legend see next page.)

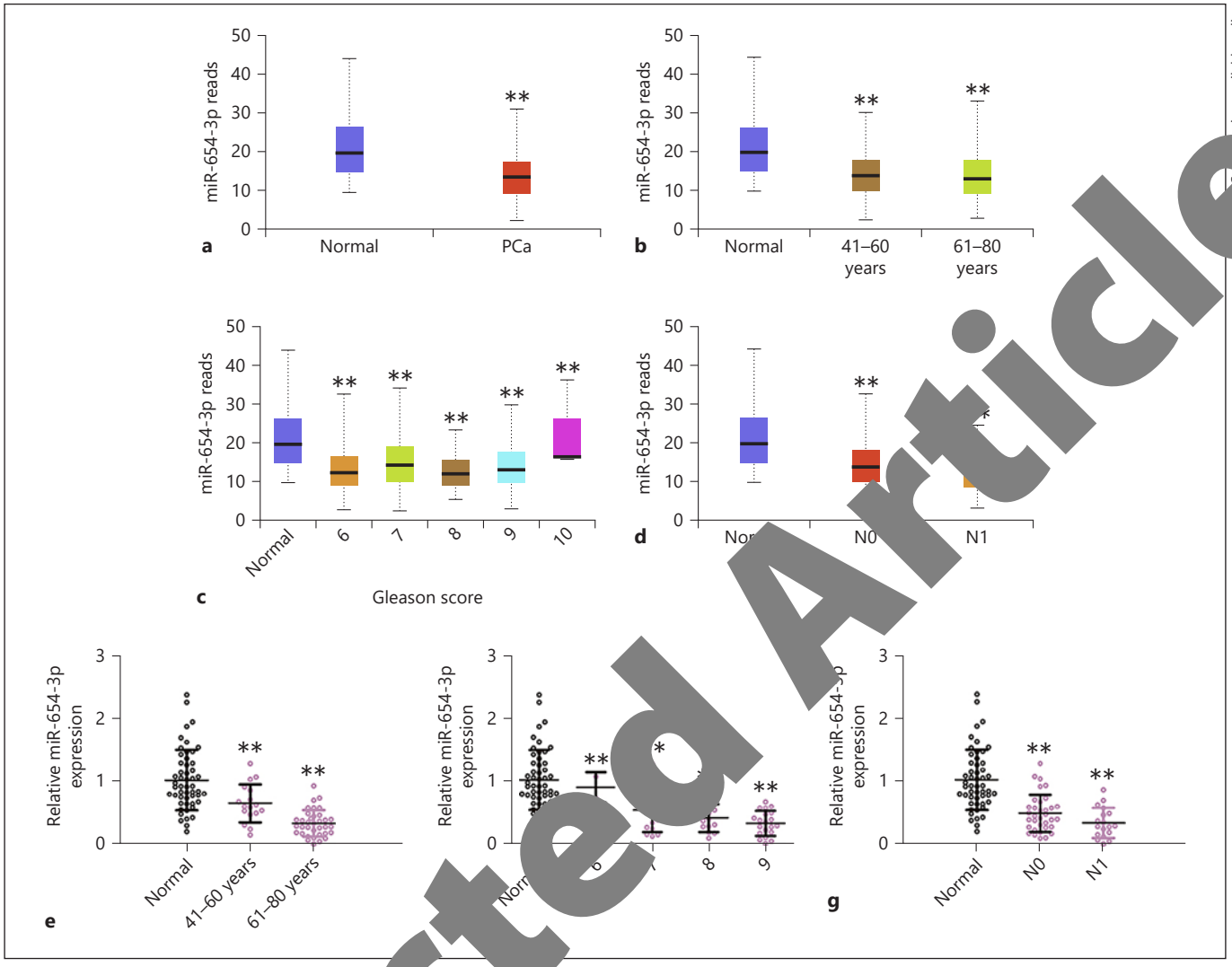

Fig. 3. Correlation between clinical/histopathological data and miR-654-3p in PCa based on the TGCA and our own cohort. **a** TCGA database was used to determine miR-654-3p expression in PCa tissues. **b–d** Using TCGA database, the correlation between miR-654-3p expression and age, Gleason score, and lymph node metastasis was evaluated in patients with PCa. **e–g** Using our own cohort, the correlation between miR-654-3p expression and age, Gleason score, and lymph node metastasis was evaluated in patients with PCa. $^{**}p < 0.01$. TCGA, The Cancer Genome Atlas; PCa, prostate cancer; miR-654-3p, microRNA-654-3p.

Fig. 2. LIPE-AS1 functions as an miR-654-3p sponge in PCa cells. **a** The subcellular distribution of LIPE-AS1 was predicted using lncLocator. **b** The subcellular fractionation assay confirmed the localization of LIPE-AS1 in 22RV1 and DU145 cells. **c** Ten miRNAs predicted binding capacity for LIPE-AS1. **d** After LIPE-AS1 silencing, qRT-PCR was conducted to determine the levels of the top 10 miRNAs (miR-660, miR-654-3p, miR-642a-5p, miR-520a-5p, miR-455-5p, miR-424-5p, miR-330-5p, miR-326, miR-299-3p, and miR-107) in 22RV1 and DU145 cells. **e** The expression of miR-654-3p in 52 pairs of PCa tissues and adjacent normal tissues was evaluated via qRT-PCR. **f** Pearson's correlation analysis revealed the correlation between the expressions of miR-654-3p and LIPE-AS1 in the 52 PCa tissues. **g** The predicted wild-type and mutant-binding sites between LIPE-AS1 and miR-654-3p are presented. **h** Luciferase reporter assay was performed to verify the binding sites for LIPE-AS1 and miR-654-3p in 22RV1 and DU145 cells. **i** RIP assay was performed to detect the enrichment of LIPE-AS1 and miR-654-3p in anti-IgG or anti-Ago immunoprecipitation of 2RV1 and DU145 cells. **j** PCa cells were transfected with bio-miR-654-3p or bio-NC. The relative enrichment of LIPE-AS1 in the yield bio-miRNA-lncRNA complexes was analyzed applying qRT-PCR. $^{**}p < 0.01$. qRT-PCR, quantitative reverse transcription polymerase chain reaction; PCa, prostate cancer; LIPE-AS1, LIPE antisense RNA 1; RIP, RNA immunoprecipitation; bio-miR-654-3p, biotinylated miR-654-3p mimic; bio-NC, biotinylated NC mimic; lncRNA, long noncoding RNA; miR-654-3p, microRNA-654-3p.

ther revealed that LIPE-AS1, miR-654-3p, and HDGF coexist in the same RNA-induced silencing complex, confirming the direct interaction between the 3 molecules in PCa cells (shown in Fig. 5c). Anti-miR-654-3p was used in the rescue experiments, and its efficiency in silencing miR-654-3p expression was confirmed via qRT-PCR (shown in Fig. 5d). Anti-miR-654-3p or anti-NC and si-LIPE-AS1 were transfected into 22RV1 and DU145 cells. The expression levels of miR-654-3p were upregulated in LIPE-AS1-silenced 22RV1 and DU145 cells; this trend was mitigated after miR-654-3p inhibition (shown in Fig. 5e). qRT-PCR and Western blotting results demonstrated that si-LIPE-AS1 transfection suppressed the mRNA and protein expression levels of HDGF in 22RV1 and DU145 cells; however, cotransfection with anti-miR-654-3p rescued the expression of HDGF after LIPE-AS1 knockdown (shown in Fig. 5f, g). Moreover, Pearson's correlation analysis revealed a positive correlation between LIPE-AS1 and HDGF in PCa tissues (shown in Fig. 5h). Taken together, these results demonstrate that LIPE-AS1 acts as a ceRNA in PCa cells by sequestering miR-654-3p, leading to increased HDGF expression.

LIPE-AS1 Promotes the Malignancy of PCa Cells by Targeting the miR-654-3p/HDGF Axis

Given that LIPE-AS1 positively modulated HDGF expression in PCa cells by sequestering miR-654-3p, [illegible] experiments were additionally performed to explore whether LIPE-AS1 exerted its roles in PCa [illegible] by targeting the miR-654-3p/HDGF axis. After transfecting 22RV1 and DU145 cells with anti-miR-654-3p, anti-NC and si-LIPE-AS1, cell proliferation, migration, and invasion were evaluated. Anti-miR-654-3p cotransfection rescued the inhibition [illegible] proliferation of 22RV1 and DU145 cells triggered [illegible] silencing (shown in Fig. 6a). Furthermore, miR-654-3p inhibition blocked the inhibitory action of si-LIPE-AS1 on the migration (shown in Fig. 6b) and invasive (shown in Fig. 6c) abilities of 22RV1 and DU145 cells.

22RV1 and DU145 cells were transfected with si-LIPE-AS1 and pcDNA3.1-HDGF or pcDNA3.1. First, the protein expression level of HDGF in pcDNA3.1-HDGF transfected or pcDNA3.1-transfected 22RV1 [illegible] DU145 cells was measured. The results indicated successful overexpression efficacy (shown in Fig. 6d). LIPE-AS1 interference suppressed 22RV1 and DU145 cell proliferation; the antiproliferative effects were offset by HDGF upregulation (shown in Fig. 6e). Similarly, Transwell migration and invasion assays revealed that LIPE-AS1 loss decreased the migration (shown in Fig. 6f) and invasive (shown in Fig. 6g) abilities of 22RV1 and DU145 cells; however, reintroduction of HDGF prevented this inhibition. In summary, these results suggest that LIPE-AS1 promotes the malignant phenotype of PCa cells by sequestering miR-654-3p and thereby increasing HDGF expression.

LIPE-AS1 Depletion Impedes the Tumor Growth of PCa Cells in vivo

To investigate the role of LIPE-AS1 on tumor growth in vivo, DU145 cells stably expressing sh-LIPE-AS1 or sh-NC were subcutaneously injected into nude mice. The transplanted tumors derived from sh-LIPE-AS1-expressed DU145 cells were smaller (shown in Fig. 7a) and had slower growth rate (shown in Fig. 7b) than those derived from sh-NC-expressed cells. In addition, the tumor weight was lower in the sh-LIPE-AS1-injected group than that in the sh-NC group (shown in Fig. 7c). After tumor excision, the levels of LIPE-AS1, miR-654-3p, and HDGF were determined in the transplanted tumors. The expression levels of LIPE-AS1 (shown in Fig. 7d) and HDGF

Fig. 4. miR-654-3p exerts tumor-inhibiting roles and directly targets HDGF in PCa. **a** qRT-PCR was conducted to determine the expression of miR-654-3p in 22RV1 and DU145 cells after transfecting the cells with miR-654-3p mimic or NC mimic. **b** CCK-8 assay was used to examine the proliferation of 22RV1 and DU145 cells after transfection with miR-654-3p mimic or NC mimic. **c**, **d** After miR-654-3p expression, the migration, and invasive abilities of 22RV1 and DU145 cells was analyzed using the Transwell migration and invasion assays (×200 magnification). **e** Predicted binding sites for miR-654-3p in the 3′-untranslated regions of HDGF. The mutant binding sequences are also presented. **f** qRT-PCR analysis was used to determine the mRNA expression level of HDGF in the 52 pairs of PCa tissues and adjacent normal tissues. **g** Correlation between the expression of HDGF and miR-654-3p in the 52 PCa tissues was studied using Pearson's correlation analysis. **h**, **i** The mRNA and protein levels of HDGF were measured via qRT-PCR and Western blotting, respectively, in 22RV1 and DU145 cells after transfection with miR-654-3p mimic or NC mimic. **j** The luciferase reporter assay was conducted to measure the luciferase activity in 22RV1 and DU145 cells after cotransfection with miR-654-3p mimic or NC mimic and HDGF-wt or HDGF-mut. $^{**}p < 0.01$. HDGF, hepatoma-derived growth factor; PCa, prostate cancer; qRT-PCR, quantitative reverse transcription polymerase chain reaction; miR-654-3p, microRNA-654-3p; NC, negative control; wt, wild-type; mut, mutant.

(For figure see next page.)

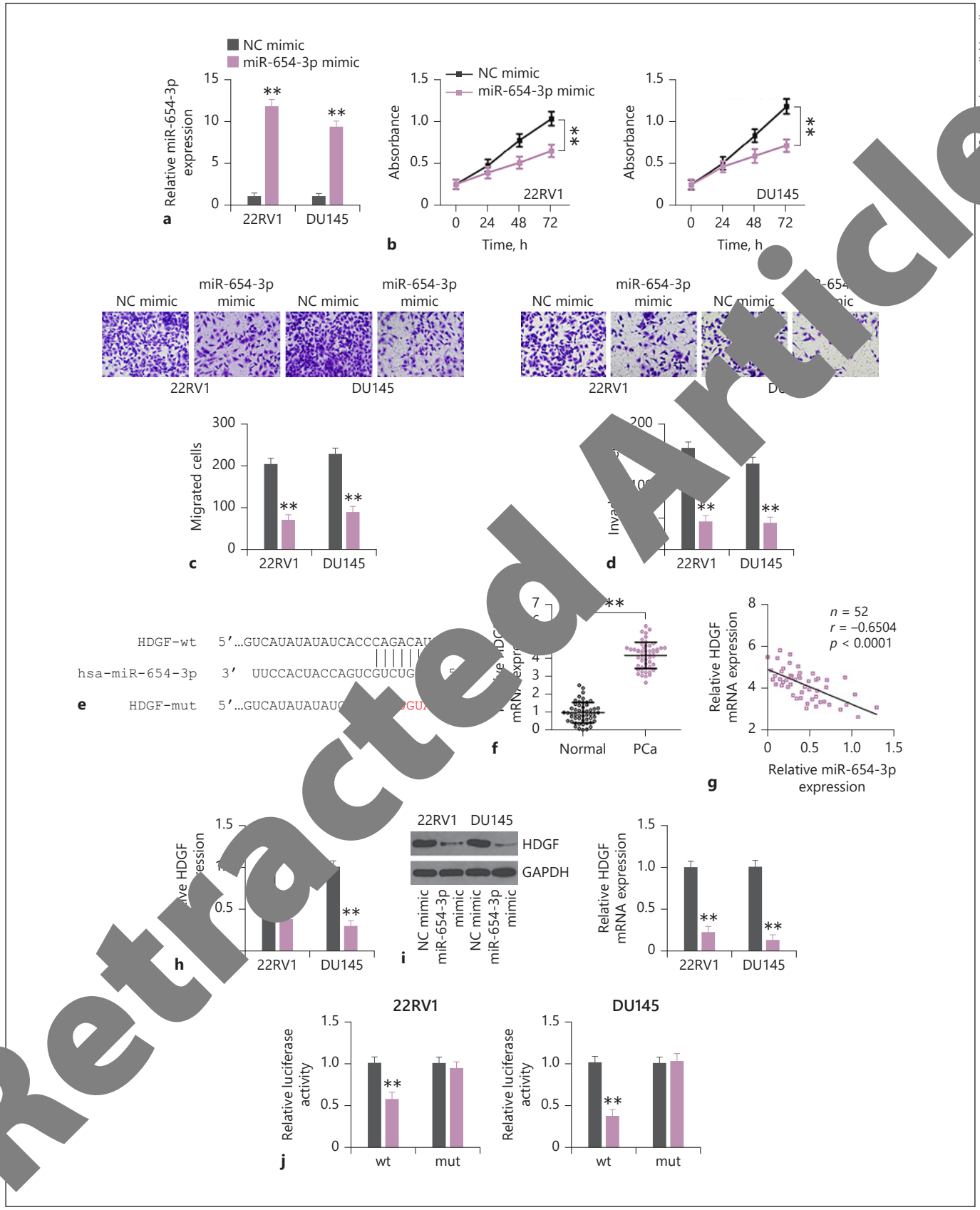

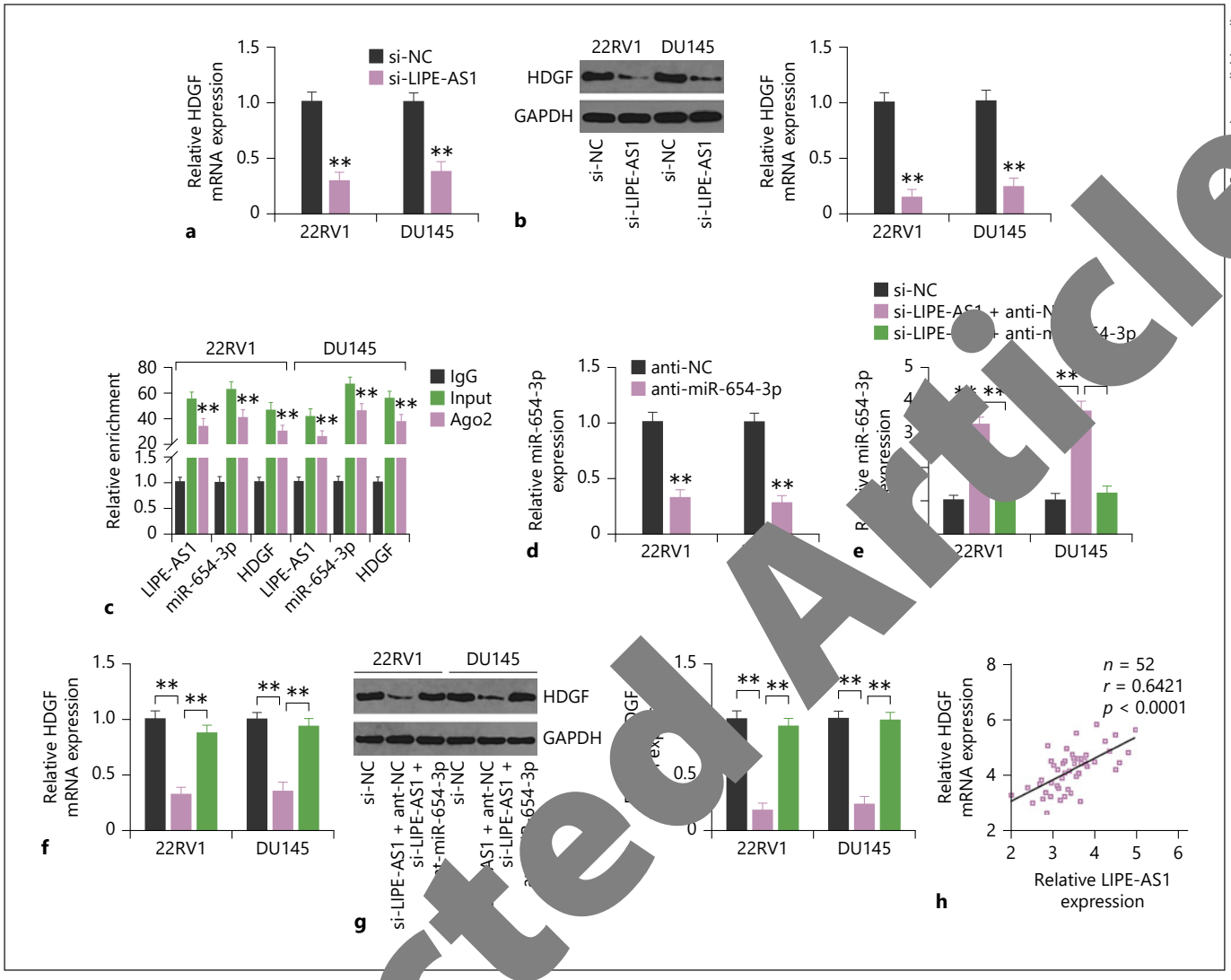

Fig. 5. LIPE-AS1 acts as a ceRNA by adsor miR -3p to up-regulate HDGF in PCa cells. **a**, **b** T RN otein expression levels of HDGF in si-LIPE fected or si-NC-transfected 22RV1 and DU145 cell er using qRT-PCR and Western blotting, respecti y. **c** R ssa as conducted to detect the enrichment of LIPE A miR , and HDGF in an RNA-induced silencing com Relative miR-654-3p expression was confirmed in and 45 cells after anti-miR-654-3p or anti-NC injec LIPE- epleted 22RV1 and DU145 cells were further t d with anti-miR-654-3p or anti-NC. The expression of miR-654-3p was determined using qRT-PCR. **f**, **g** qRT-PCR and Western blotting were used to measure the mRNA and protein expression levels of HDGF, respectively, in the aforementioned cells. **h** Pearson's correlation analysis revealed the relationship between LIPE-AS1 and HDGF in PCa tissues. $^{**}p < 0.01$. LIPE-AS1, LIPE antisense RNA 1; ceRNA, competing endogenous RNA; HDGF, hepatoma-derived growth factor; PCa, prostate cancer; qRT-PCR, quantitative reverse transcription polymerase chain reaction; miR-654-3p; microRNA-654-3p; NC, negative control; RIP, RNA immunoprecipitation.

owi 7e) were remarkably decreased, whereas 54-3p expression (shown in Fig. 7f) was increased in t -LIPE-AS1-injected tumor xenografts. Taken together, LIPE-AS1 knockdown hinders the tumor growth Ca cells in vivo.

Discussion

In recent years, a number of lncRNAs have been revealed to play crucial regulatory roles in the oncogenesis and progression of PCa [19]. Therefore, studying the roles and mechanisms of action of lncRNAs would

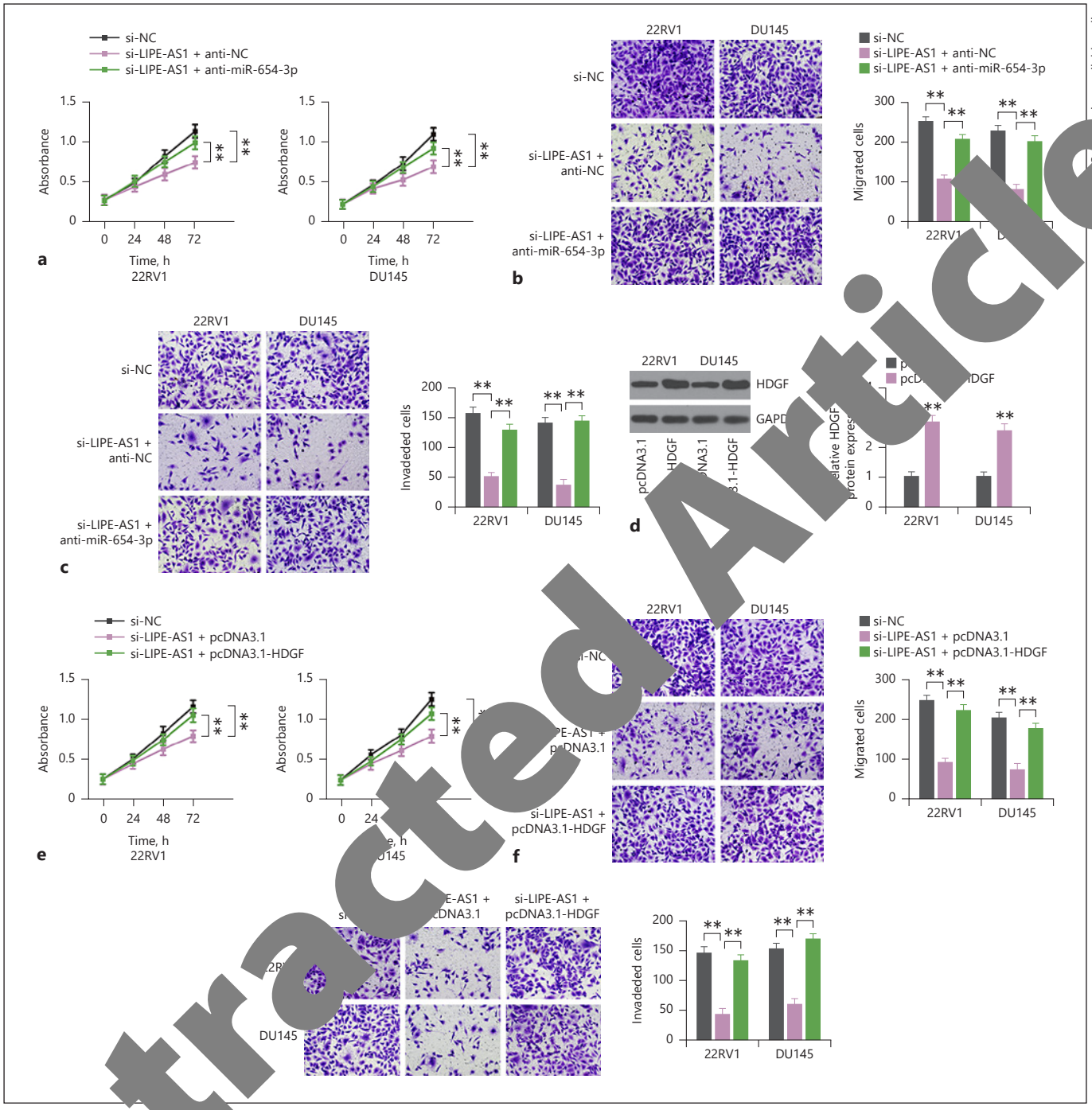

Fig. 6. [illegible]lated miR-654-3p or overexpressed HDGF mitigates [illegible]mediated effects on the proliferation, migration, a[illegible]of PCa cells. **a** 22RV1 and DU145 cells were transfe[illegible]h si-LIPE-AS1 and anti-miR-654-3p or anti-NC. CCK-8 assay was performed to determine cell proliferation. [illegible]well migration and invasion assays were performed to assess the migration and invasive abilities of 22RV1 and DU145 [illegible] treated as described above (×200 magnification). **d** Western [illegible]otting examined the protein expression level of HDGF in 22RV1 and DU145 cells after pcDNA3.1-HDGF or pcDNA3.1 transfection. **e** CCK-8 assay detected the proliferation ability of 22RV1 and DU145 cells after transfection with si-NC, si-LIPE-AS1 + pcDNA3.1, or si-LIPE-AS1 + pcDNA3.1-HDGF. **f**, **g** Transwell migration and invasion assays were conducted to determine the cell migration and invasive abilities of 22RV1 and DU145 cells after co-transfection with si-LIPE-AS1 and pcDNA3.1-HDGF or pcDNA3.1 (×200 magnification). $^{**}p < 0.01$. HDGF, hepatoma-derived growth factor; miR-654-3p, microRNA-654-3p; CCK-8, Cell Counting Kit 8; si-LIPE-AS1, small interfering RNAs against LIPE-AS1; LIPE-AS1, LIPE antisense RNA 1.

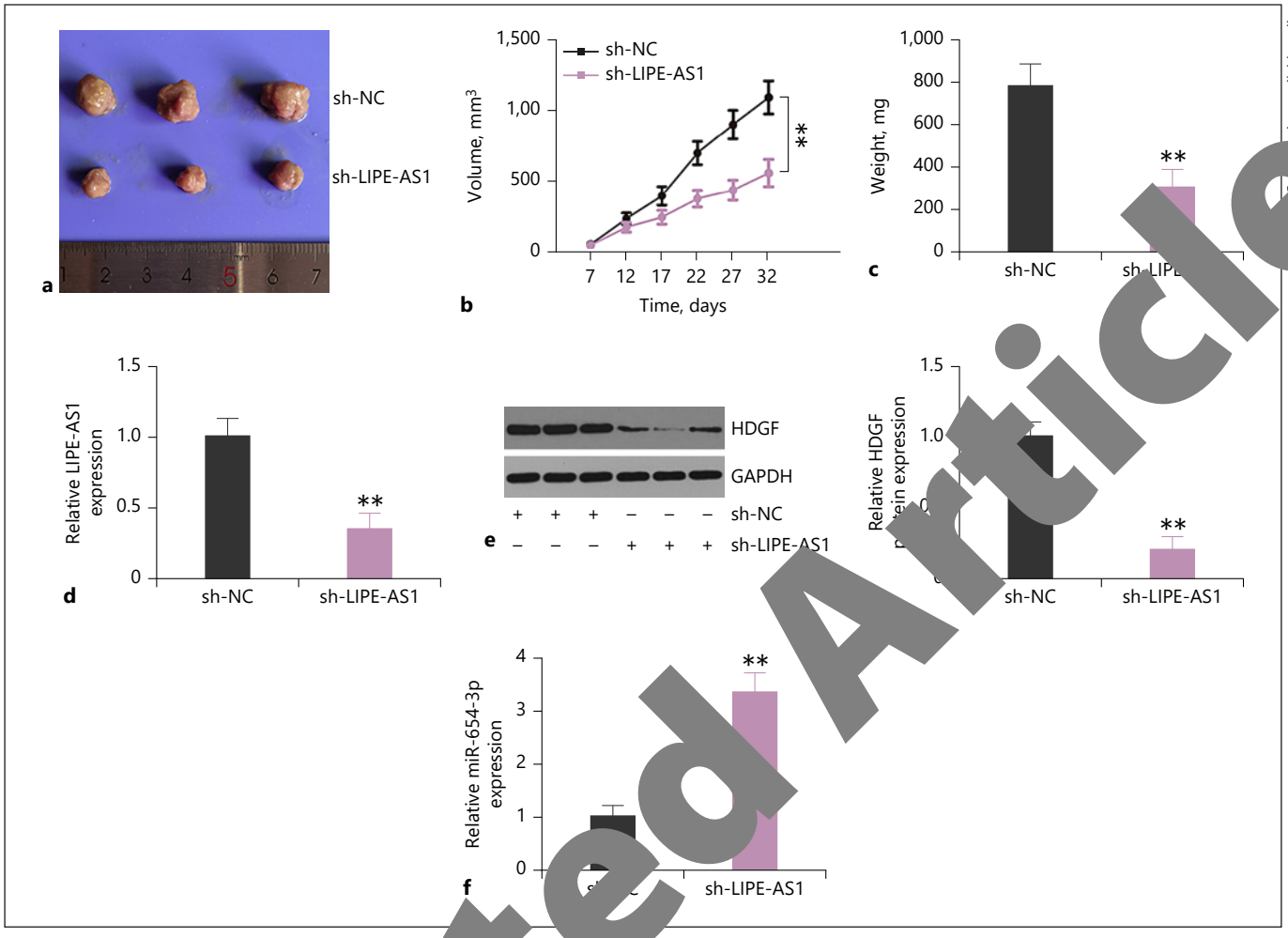

Fig. 7. LIPE-AS1 knockdown inhibits PCa tumorigenesis in vivo. **a** Images of the transplanted tumors in nude mice injected with sh-LIPE-AS1- or sh-NC-transfected SW1545 cells after being resected. **b** Growth curves of the transplanted tumors from nude mice in the sh-LIPE-AS1 and sh-NC groups. **c** Weight of the tumor xenografts obtained from the 2 groups. **d**, **e** Expression levels of LIPE-AS1 and HDGF in xenografts were determined via qRT-PCR and Western blotting, respectively. **f** qRT-PCR results showed the expression levels of miR-654-3p in tumor xenografts of mice in the sh-LIPE-AS1 and sh-NC groups. $^{**}p < 0.01$. LIPE-AS1, LIPE antisense RNA 1; PCa, prostate cancer; sh-LIPE-AS1, short hairpin RNA against the expression of LIPE-AS1; sh-NC, short hairpin RNA negative control; HDGF, hepatoma-derived growth factor; qRT-PCR, quantitative reverse transcription polymerase chain reaction; miR-654-3p, microRNA-654-3p.

help identify the novel targets for PCa treatment. Despite the vast number of lncRNAs verified in the human genome, the specific functions of lncRNAs in the processes of oncogenicity and downstream signaling pathways in PCa remain poorly understood. In this study, we determined the expression pattern of LIPE-AS1 in PCa. The detailed roles of LIPE-AS1 were investigated in vitro and in vivo. In addition, the mechanisms underlying the oncogenic roles of LIPE-AS1 in PCa were confirmed to provide a novel insight into and a new mechanism underlying PCa pathogenesis.

Various studies have focused on lncRNAs in PCa. For example, LINC00173 [20] and PROX1-AS1 [21] are overexpressed in PCa and function as oncogenes. On the other hand, LINC00261 [22] and TUG1 [23] are downregulated in PCa and inhibit PCa progression. However, whether LIPE-AS1 is involved in PCa malignancy remains unknown. Evidence suggests that LIPE-AS1 is highly expressed in PCa; this is consistent with the results of TCGA database. PCa patients manifesting high LIPE-AS1 expression had shorter overall survival than those manifesting low LIPE-AS1 expression. Downregulated LIPE-

AS1 resulted in a notable decrease in PCa cell proliferation, migration, and invasion in vitro. Furthermore, loss of LIPE-AS1 decreased the tumor growth of PCa cells in vivo. In summary, our results demonstrated the enhanced expression and pro-oncogenic roles of LIPE-AS1 in PCa.

Subsequently, we elucidated the downstream mechanism of action of LIPE-AS1 in PCa cells. Mechanically, the widely studied latent mechanism of action of lncRNAs is dependent on their subcellular location. lncRNAs located in the nucleus are capable of directly binding to proteins and modulating gene expression at the transcriptional level [17]. On the other hand, cytoplasmic lncRNAs harbor an miRNA response element, which can competitively bind to certain miRNAs and regulate their target genes at the posttranscriptional level, thereby functioning as ceRNAs [24]. Our study demonstrated that LIPE-AS1 was primarily distributed in the cytoplasm of PCa cells, suggesting that LIPE-AS1 is a ceRNA. Using a reliable online predicting tool, miR-654-3p was identified as a potential downstream miRNA target of LIPE-AS1 in PCa. We demonstrated that LIPE-AS1 depletion resulted in an increased expression level of miR-654-3p in PCa cells. Consistent with the findings of a recent study [25], miR-654-3p was weakly expressed in PCa cells, manifesting an inverse expression correlation with LIPE-AS1. We confirmed the direct interaction between LIPE-AS1 and miR-654-3p in PCa cells using the luciferase report[er] RIP assays. Taken together, these results show tha[t LIP]E-AS1 acts as a miR-654-3p sponge in PCa [cells].

miR-654-3p is underexpressed in p[ancreat]ic cancer [26] and non-small-cell lung cancer [27]. [How]ever, it is upregulated in gastric cancer [28] and ovari[an] cancer [29]. In particular, miR-654-3p is ex[pre]ssed at low levels in PCa and controls tumor cell gro[wth] and metastasis [25]. Previously, multiple [genes], including AKT3 [29], SYTL2 [30], QPRT [31], a[nd] PR[KD1] are confirmed as direct targets of miR-654-3p [in] human cancers. These genes may also be [im]portant [in] PCa and require further explora[tion]. In [the] present study, we verified that HDGF is t[he] direct ta[rget] and functional mediator of miR-654-3p [in] cells. Subsequently, our data proved that LIP[E-AS]1 de[ple]tion upregulated HDGF in PCa cells by ad[sorb]ing miR-654-3p. The RIP assay further corroborate[d] the co[-exi]stence of LIPE-AS1, miR-654-3p, and HDGF [in] the same RNA-induced silencing complex. Accordingly, for the first time, we demonstrated that LIPE-AS1, miR-654-3p, and HDGF constitute a novel ceRNA pathway in PCa.

HDGF, a heparin-binding growth factor, is located on chromosome 1 in the q21–q23 region. The tumor-promoting roles of HDGF in PCa tumorigenesis and progression have been unveiled in previous studies [32]. At present, our results demonstrate that the HDGF level positively correlates with LIPE-AS1 levels in PCa tissues. Moreover, rescue assays confirmed that miR-654-3p downregulation or HDGF overexpression weakens the actions of LIPE-AS1 depletion on cell proliferation, migration, and invasion in PCa cells. In other words, our research uncovers the functions of the LIPE-AS1/miR-654-3p/HDGF ceRNA pathway in promoting tumor processes of PCa.

Our study has 2 limitations. First, the clinical cohort is very small. Second, our current research only focused the effect of LIPE-AS1 depletion on the tumor growth of PCa cells in vivo; but, the influence of LIPE-AS1 knockdown on tumor metastasis in vivo was not tested. In the near future, we will collect more tissue samples and further verify the observations in this study. Also, in vivo experiments will be supplemented to address the involvement of LIPE-AS1 in tumor metastasis.

In conclusion, our study demonstrated that LIPE-AS1 is upregulated in PCa and is significantly associated with overall survival. LIPE-AS1 is a ceRNA functioning as a sponge for miR-654-3p in PCa cells, which enhances HDGF expression and promotes cancer progression. The identified LIPE-AS1/miR-654-3p/HDGF ceRNA pathway contributes to PCa pathogenesis and targeting this pathway may have therapeutic potentials.

Statement of Ethics

This study was approved by the Research Ethics Committee of the First Affiliated Hospital of Qiqihar and was conducted in full accordance with the World Medical Association's Declaration of Helsinki. All participants signed an informed consent document before the study. All animal procedures were approved by the Animal Care and Use Committee of the First Affiliated Hospital of Qiqihar and were conducted in compliance with the recommended procedures of National Institutes of Health guidelines for the care and use of laboratory animals.

Conflict of Interest Statement

The authors declare that they have no competing interests.

Funding Sources

The authors did not receive any funding for this study.

Author Contributions

All the authors have made significant contribution to the findings and methods. They have read and approved the final draft.

Availability of Data and Material

The datasets used and/or analyzed during the present study are available from the corresponding author upon reasonable request.

References

1 Ferlay J, Colombet M, Soerjomataram I, Mathers C, Parkin DM, Piñeros M, et al. Estimating the global cancer incidence and mortality in 2018: GLOBOCAN sources and methods. Int J Cancer. 2019 Apr 15;144(8):1941–53.

2 Tian JY, Guo FJ, Zheng GY, Ahmad A. Prostate cancer: updates on current strategies for screening, diagnosis and clinical implications of treatment modalities. Carcinogenesis. 2018 Mar 8;39(3):307–17.

3 Bray F, Ferlay J, Soerjomataram I, Siegel RL, Torre LA, Jemal A. Global cancer statistics 2018: GLOBOCAN estimates of incidence and mortality worldwide for 36 cancers in 185 countries. CA Cancer J Clin. 2018 Nov;68(6):394–424.

4 Litwin MS, Tan HJ. The diagnosis and treatment of prostate cancer: a review. JAMA. 2017 Jun 27;317(24):2532–42.

5 Shepard DR, Raghavan D. Innovations in the systemic therapy of prostate cancer. Nat Rev Clin Oncol. 2010 Jan;7(1):13–21.

6 Cornford P, Bellmunt J, Bolla M, Briers E, De Santis M, Gross T, et al. EAU-ESTRO-SIOG guidelines on prostate cancer. Part II: treatment of relapsing, metastatic, and castration-resistant prostate cancer. Eur Urol. 2017 Apr;71(4):630–42.

7 Schmitz-Drager BJ, Muhlich S, Lange C, Benderska-Soder N, Bismarck E, Starlinger R, et al. Effectiveness and distribution of testosterone levels within first year of androgen deprivation therapy in a real-world setting: results from the non-interventional German Coho LEAN Study. Urol Int. 2021 Feb 25;1–10.

8 Attard G, Parker C, Eeles RA, Schröder F, Tomlins SA, Tannock I, et al. Pro r. Lancet. 2016 Jan 2;387(10013):

9 Chen Y, Lan T. Molecular orig , e ess regulation, and biological ction nd gen receptor splicing t 7 i e cancer. Urol Int. 202 1–17.

10 Ulitsky I, P P. li s: genomics, evolution, a hanisms 2013 Jul 3;154(1):26–4

11 Kleaveland B, Shi o J, Bartel DP. A netw codi gulatory RNAs acts in ma ian brain. Cell. 2018 Jul 12;174 62

Che The physiological function of long oding RNAs. Noncoding RNA 2020 Dec;5(4):178–84.

13 Misawa A, Takayama KI, Inoue S. Long noncoding RNAs and prostate cancer. Cancer Sci. 2017 Nov;108(11):2107–14.

14 Adams BD, Kasinski AL, Slack FJ. Aberrant regulation and function of microRNAs in cancer. Curr Biol. 2014 Aug 18;24(16):R762–76.

15 Bartel DP. MicroRNAs: genomics, biogenesis, mechanism, and function. Cell. 2004 Jan 23;116(2):281–97.

16 Ghafouri-Fard S, Shoorei H, Taheri M. Role of microRNAs in the development, prognosis and therapeutic response of patients with prostate cancer. Gene. 2020 Oct 30;759:144

17 Zhang XZ, Liu H, Chen SR. Mecha long non-coding RNAs in cancers dynamic regulations. Cancers. 2020 15;12(5):1245.

18 Cao D, Wang Y, Li D, Wang L. Recons tion and analysis differentially pressed lncRNA-mi RNA netwo based on competitive en RNA in hepatocellular carcino Eukaryot Gene Expr. 2019;29 9–49.

19 Ramnarine VR, Kob , Gi A, Nouri M, Lin D, W tion of long noncodin prostate cancer initi gre ion, and its clinical ilit in ma ment. Eur Urol. 2019 5(5):

20 H, Yang , Tu L, Wang LY, Zhao XC, g non-coding RNA LINC00173 serv ge for miR-338-3p to promote prostate cancer progression via regulating Ra 5. Eur Rev Med Pharmacol Sci. 2020 Sep; 5):9290–302.

ian C, Liao CH, Tan BF, Chen YF, Dang BW, Chen JL, et al. LncRNA PROX1-AS1 promotes proliferation, invasion, and migration in prostate cancer via targeting miR-647. Eur Rev Med Pharmacol Sci. 2020 Sep;24(17):2938.

22 Li Y, Li H, Wei X. Long noncoding RNA LINC00261 suppresses prostate cancer tumorigenesis through upregulation of GATA6-mediated DKK3. Cancer Cell Int. 2020;20:474.

23 Li G, Yang J, Chong T, Huang Y, Liu Y, Li H. TUG1 knockdown inhibits the tumorigenesis and progression of prostate cancer by regulating microRNA-496/Wnt/β-catenin pathway. Anticancer Drugs. 2020 Jul;31(6):592–600.

24 Wang L, Cho KB, Li Y, Tao Gu Long noncoding RNA (lncRN diated competing endogenous R netw ro vide novel potential bi kers and peutic targ r color cancer. Int J Mol Sci. 2019 N 16;20(22)

25 Formosa A, M EK, , Italiano D, Fin zi- ro ne AJ, et al. MicroRNAs , mi , miR-376a, miR-376c, miR- , miR-487b, miR-48 p, m miR-654-3p, mapped to th q32.3 regulate proliferation, osis, migration and invasion in metastatic prostate cancer cells. Oncogene. 2014 Oct 44):5173–82.

Geral MV, Nakaya HI, Kimura ET. Down- lation of 14q32-encoded miRNAs and or suppressor role for miR-654-3p in papillary thyroid cancer. Oncotarget. 2017 Feb 7;8(6):9597–607.

27 Pu JT, Hu Z, Zhang DG, Zhang T, He KM, Dai TY. MiR-654-3p suppresses non-small cell lung cancer tumourigenesis by inhibiting PLK4. Onco Targets Ther. 2020;13:7997–8008.

28 Deng G, Mou T, He J, Chen D, Lv D, Liu H, et al. Circular RNA circRHOBTB3 acts as a sponge for miR-654-3p inhibiting gastric cancer growth. J Exp Clin Cancer Res. 2020 Jan 13;39(1):1.

29 Duan M, Fang M, Wang C, Wang H, Li M. LncRNA EMX2OS induces proliferation, invasion and sphere formation of ovarian cancer cells via regulating the miR-654-3p/AKT3/PD-L1 axis. Cancer Manag Res. 2020;12:2141–54.

30 Zhou X, Li J, Teng J, Liu Y, Zhang D, Liu L, et al. Long noncoding RNA BSN-AS2 induced by E2F1 promotes spinal osteosarcoma progression by targeting miR-654-3p/SYTL2 axis. Cancer Cell Int. 2020;20:133.

31 Niu YC, Tong J, Shi XF, Zhang T. MicroRNA-654-3p enhances cisplatin sensitivity by targeting QPRT and inhibiting the PI3K/AKT signaling pathway in ovarian cancer cells. Exp Ther Med. 2020 Aug;20(2):1467–79.

32 Shetty A, Dasari S, Banerjee S, Gheewala T, Zheng G, Chen A, et al. Hepatoma-derived growth factor: a survival-related protein in prostate oncogenesis and a potential target for vitamin K2. Urol Oncol. 2016 Nov;34(11):483–e8.